Astron. Astrophys. 322, 696–703 (1997)

ASTRONOMY
AND
ASTROPHYSICS

Electron acceleration at steepened magnetic field structures in the vicinity of quasi-parallel shock waves

H.-T. Claßen and G. Mann

Astrophysikalisches Institut Potsdam, Observatorium für solare Radioastronomie, Telegrafenberg A31, D-14473 Potsdam, Germany

Received 14 October 1996 / Accepted 5 December 1996

Abstract. The acceleration of charged particles at shock waves plays an important role in many fields of astrophysics, but only a few shocks can be observed by in-situ measurements. Extraterrestrial measurements at Earth's bow shock and interplanetary shock waves show that supercritical, quasi-parallel shock waves are accompanied by large-amplitude magnetic field fluctuations (so-called steepened wave structures) in the upstream region. Test particle calculations with modelled electric and magnetic fields of such steepened wave structures yield the acceleration of thermal electrons up to nearly relativistic velocities (kinetic energy in the keV range). For smoothly varying magnetic fields an analytical treatment is possible in the framework of adiabatic theory. These analytical calculations show that the acceleration of electrons is caused by a particle drift in the direction of the electric field due to a noncoplanar component of the magnetic field at the steepened field structures. As an application of this result the generation of solar type II radio bursts – the radio signature of electrons accelerated at coronal shock waves - is briefly discussed.

Key words: shock waves: acceleration of particles – Sun: radio radiation

1. Introduction

Shock waves play an important role in astrophysics, since they are able to accelerate particles (e.g. Fermi 1949, Axford et al. 1977). In the heliosphere shock waves appear as travelling shock waves in the solar corona and the interplanetary space, planetary bow shocks, pairs of forward and reverse shocks at corotating interaction regions and the termination shock at the outer boundary of the heliosphere. In the solar corona shock waves are generated by flares and/or coronal mass ejections (CME's). They manifest themselves as type II radio bursts (cf. Fig. 1) in dynamic radio spectra (e.g. Krüger 1979, Nelson & Melrose 1985, Auraß 1992, Mann 1995a). But other kinds of shock waves are also emitting radio waves. For instance, interplanetary type II bursts observed below 1MHz are caused by travelling interplanetary shock waves (cf. Bougeret 1985). The radio emission of Earth's bow shock is described by Filbert and Kellog (1979), Treumann et al. (1986) and Cairns (1986). Gurnett (1995) reported on some serious hints for radio radiation of the termination shock. All these radio phenomena evidently show that electrons are accelerated up to suprathermal and, partly, even up to relativistic velocities.

Holman and Pesses (1983) suggested that the energetic electrons needed for type II burst emission are produced by shock drift acceleration. Leroy and Mangeney (1984) as well as Wu (1984) showed that the accelerated electrons establish a shifted loss-cone distribution in the upstream region of the shock. Such a distribution is unstable and able to excite upper hybrid waves, which convert into radio waves (Benz & Thejappa 1988).

Mann and Claßen (1995) argued that the energetic electrons needed for the type II burst radiation can only be produced by shock drift acceleration if the shock waves are nearly perpendicular, i.e., $88^\circ \leq \theta_{Bn} \leq 90^\circ$ (θ_{Bn}, angle between the shock normal and the upstream magnetic field) under coronal circumstances. Since solar and interplanetary type II radio bursts appear for a few minutes and several hours, respectively (Nelson & Melrose 1985, Lengyel-Frey & Stone 1989), it seems doubtful whether the shock is able to keep within this small angular range for such a long time. Therefore, Mann and Claßen (1995) were motivated to search for an electron accelerating mechanism at quasi-parallel shock waves.

It is well-known from in-situ measurements at Earth's bow shock and interplanetary shocks that supercritical, quasi-parallel shock waves are accompanied by large amplitude magnetic field fluctuations (Kennel et al. 1985). Recently, so-called SLAMS (Short Large Amplitude Magnetic Field Structures) are observed as a common feature at the quasi-parallel region of Earth's bow shock (Schwartz et al. 1992). They are strong magnetic field compressions within a spatial range of 10 ion inertial lengths (Schwartz et al. 1992, Mann et al. 1994). Mann and Claßen (1995) proposed a mechanism which allows to accelerate electrons to subrelativistic velocities by multiple encounters between two approaching SLAMS.

Send offprint requests to: H.-T. Claßen

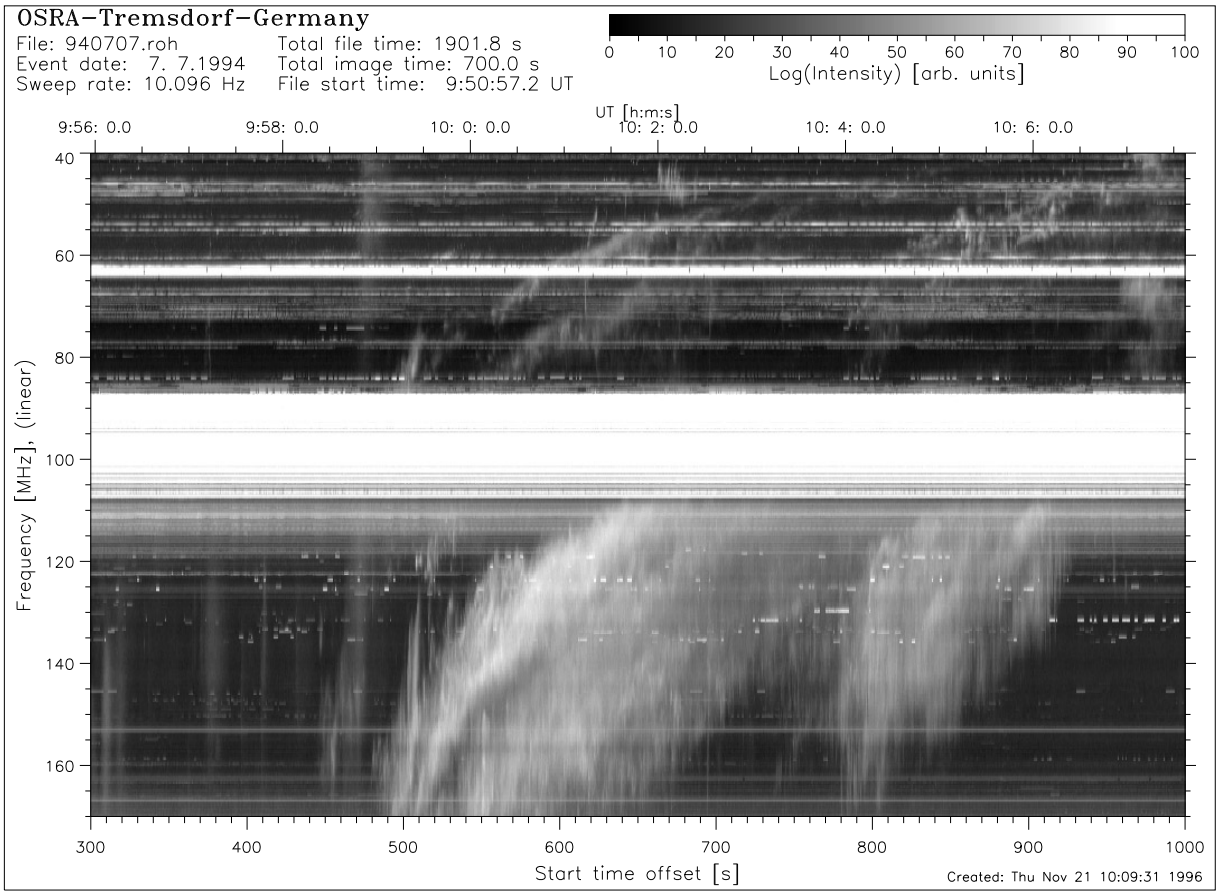

Fig. 1. Dynamic radio spectrum of a solar type II radio burst occuring on July 7, 1994 showing different fine structures: Fundamental-harmonic structure, "backbones" , multiple-lane structures (the single slowly drifting bands) and "herringbones" (for further explanations see text). The horizontal lines are due to terrestrial transmitters (measurement of the radio spectrograph of the Astrophysikalisches Institut Potsdam in Tremsdorf).

Electrons accelerated at coronal shock waves can indirectly be studied analysing solar type II radio bursts (e.g. Nelson & Melrose 1985). In general, a solar type II burst appears as an ensemble of slowly drifting bands of enhanced radio emission in dynamic radio spectra (see Fig. 1). The well known fine structures of a type II burst are shown in Fig. 1. "Fundamental-harmonic-structure" means that the radio emission of the fundamental band (e.g. the faint radio emission in the frequency range 40-90 MHz between 09:59 and 10:03 UT) appears also with a doubled frequency (in our case even with a higher intensity) at nearly the same time. The "backbones" are the slowly drifting ($D_f \approx -0.1$ MHz/s), broad ($\Delta f/f \approx 0.3$) main emission bands. The "herringbones" are fast drifting ($D_f \approx \pm 10$ MHz/s) narrow band appendices shooting up at both sides of the backbone (observed at the harmonic band e.g. at time offsets 500 and 800 s). The herringbones are interpreted as highly energetic electrons accelerated at the shock wave (Roberts 1959). The high drift rate of this structure corresponds to the velocity of the accelerated electrons, while the slow drift of the backbone corresponds to the velocity of the shock wave in the solar corona. While the acceleration of electrons by multiple encounters between two approaching SLAMS was made responsible for the generation of the herringbones (Mann & Claßen 1995) we want to demonstrate in this paper that electrons can be accelerated up to high energies within an individual SLAMS by analysing test particle trajectories of electrons at modelled SLAMS.

A more detailed description of SLAMS will be given in the next section. The analysis of test particle trajectories of electrons at mathematically modelled SLAMS follows in Sect. 3. There it is shown that electrons can be accelerated inside single SLAMS. In order to get a better understanding of this acceleration process, we will present an analytical treatment based on the adiabatic motion of particles in smoothly varying magnetic fields. As a possible application we will discuss the generation of the fine structures of solar type II radio bursts, i.e., backbone fine structures, bandsplitting and the patchy multiple-lane structures (Sect. 4). Thus, we will be able to give a type II theory consistent with the observations, where the radio burst exciting shock wave is assumed to be a quasi-parallel one.

2. Magnetic field structures at quasi-parallel shock waves

The bow shock of the Earth is the best investigated collisionless shock in space plasmas wave. Because of its curvature it has

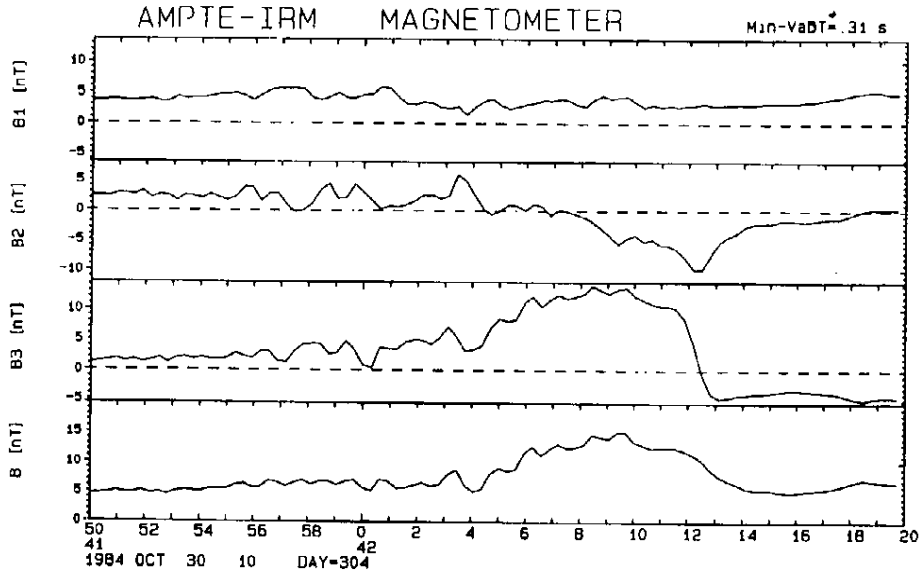

Fig. 2. Behaviour of the magnetic of a typical isolated SLAMS occuring on October 30, 1984. The first three panels show the magnetic field components in a minimum variance frame, the fourth panel shows the magnitude of the magnetic field (measurement of the AMPTE/IRM satellite).

quasi-perpendicular and quasi-parallel regions. In the upstream region of the quasi-parallel bow shock a variety of magnetic field and particle phenomena has been observed by a great number of satellite missions. Different populations of ions backstreaming from the shock are associated with low-frequency magnetohydrodynamic waves (ULF-waves) (Paschmann et al. 1979, Hoppe et al. 1981). Further observations showed hot diamagnetic cavities, hot flow anomalies and magnetic pulsations (Greenstadt et al. 1970, Schwartz et al. 1988). All these upstream phenomena are often observed and seem to be closely related (Thomsen et al. 1990).

The magnetic field structures discussed in this paper, the aforementioned SLAMS, has been characterized by Schwartz et al. (1992) as well-defined single magnetic structures with large amplitudes of about 2 or more times the background field and short durations of typically 10s (see Fig. 2). They seem to grow from the well-known ULF-waves. Schwartz & Burgess (1991) argued that a quasi-parallel shock transition should be regarded as a patchwork of ULF-waves and SLAMS, which are gradually decelerating the solar wind and subsequently forming the downstream state.

Fig. 2 shows magnetic field data of a typical SLAMS sampled by the magnetometer on board the AMPTE/IRM satellite (Lühr et al. 1985). The magnetic field components are displayed in a minimum variance system, which will be referred to later as b_x-, b_y- and b_z-component. A statistical analysis of 18 such structures was carried out by Mann et al. in 1994. They showed that SLAMS have typical amplitudes of 2.6 ± 1.2 times the ambient magnetic field. Furthermore SLAMS are associated with a density enhancement of 2.3 ± 0.8 times the unperturbed value.

SLAMS are propagating quasi-parallel to the undisturbed upstream magnetic and develop as follows: Supra-thermal diffuse ions in the far upstream region generate ULF-waves propagating along the ambient magnetic field lines. Because of the supersonic plasma flow the ULF-waves are convected back towards the shock transition and during their approach they steepen into so-called "shocklets" and SLAMS. This scenario is confirmed by two-dimensional hybrid simulations (Scholer 1993). Both the observations and simulations show that ULF-waves and SLAMS can be considered as quasi-planar structures (Scholer et al. 1992, Mann et al. 1994). SLAMS have a typical width of 10 ion inertial lengths, where the ion inertial length is given by $d_i = c/\omega_{pp}$ (c, speed of light, $\omega_{pp} = ((e^2 N_p)/(m_p \epsilon_0))^{1/2}$, proton plasma frequency, with N_p as particle number density of the protons and m_p as proton mass).

An analytical approach concerning the proporties and behaviour of ULF-waves and SLAMS using non-linear MHD wave theory was tackled by Malara & Elaoufir (1991) and Mann (1995b). This investigations showed that SLAMS can be regarded as simple magnetohydrodynamic waves, i.e., the magnetic field components can be described as functions of the form $b_i = f_i(x - V_{SL}t)$, where V_{SL} is the propagation velocity of the SLAMS.

In the following section the electron dynamics in this kind of field structures will be discussed in form of test particle calculations. Here it is worth mentioning that we are looking for acceleration mechanisms of electrons and that these processes cannot be found by hybrid simulations, where the electrons are treated as a neutralizing fluid. On the other hand it should be clear that the fraction of accelerated particles is not allowed to be too great in order to avoid the influence of accelerated particles on the given electric and magnetic fields.

3. Electron dynamics at steepened wave structures

In general, test particle calculations can provide useful insight into zeroth-order particle behaviour and into sources of free energy to drive instabilities (e.g. Decker 1988, as a review). Therefore, we have to solve the equation of motion for single particles in given electric and magnetic fields of SLAMS

$$m_e \frac{d\boldsymbol{v}}{dt} = -e(\boldsymbol{E} + \boldsymbol{v} \times \boldsymbol{B}) \,. \tag{1}$$

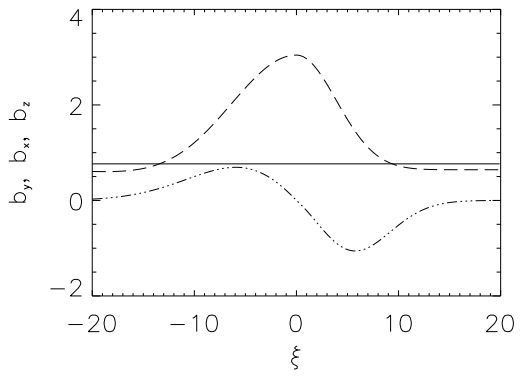

Fig. 3. Mathematically modelled magnetic field components of a single SLAMS in the SLAMS rest frame, the field components (b_x solid, b_y dashed-dotted, b_z dashed line) are normalized to the unperturbed background magnetic field and the spatial dimensions are normalized to the ion inertial length.

In order to produce the typical magnetic field structures of SLAMS we took mathematically modelled SLAMS in form of simple MHD-waves (Mann 1995b), i.e., magnetic field components $b_i = f_i(\xi)$ ($\xi := x - V_{SL}t$) resembling the field measurements of Fig. 2. An example is given in Fig. 3 where we used Gaussian functions to describe the steepening of ULF-waves

$$\begin{aligned} b_{SLx} &= \cos\psi \\ b_{SLy} &= b_{\max} p f(\xi) \\ &= b_{\max} p \begin{cases} \exp(-(\xi/L_1)^2)\sin(k\xi) & \text{if } \xi \geq 0 \\ \exp(-(\xi/L_2)^2)\sin(k\xi) & \text{if } \xi < 0 \end{cases} \\ b_{SLz} &= \sin\psi + b_{\max} g(\xi) \\ &= \sin\psi + b_{\max} \begin{cases} \exp(-(\xi/L_1)^2)\cos(k\xi) & \text{if } \xi \geq 0 \\ \exp(-(\xi/L_2)^2)\cos(k\xi) & \text{if } \xi < 0 \end{cases} . \end{aligned} \quad (2)$$

Here ψ (with $0° \leq \psi \leq \theta_{Bn} \leq 45°$) denotes the angle between the propagation direction of the SLAMS and the unpertubed magnetic field. $b_{\max}$ is the maximum magnetic field compression and p (with $|p| \leq 1$) denotes the polarisation of the SLAMS. The scales L_1 and L_2 in the functions $f(\xi)$ and $g(\xi)$ are introduced to produce the asymmetric behaviour of the steepened waves. The magnetic field has been normalized to the background magnetic field B_0 and the spatial dimensions are normalized to the ion inertial length. In Fig. 3 we chose $L_1 = 8$, $L_2 = 12$ and $k = 0.1$.

The electric field induced by the motion of the SLAMS (in the plasma rest frame) can be computed using Maxwell's equation $\nabla \times \boldsymbol{E} = -\partial \boldsymbol{B}/\partial t$, yielding $-\partial_x E_z = -\partial_t B_y$ and $\partial_x E_y = -\partial_t B_z$, with $\partial_x = \partial/\partial x$ and $\partial_t = \partial/\partial t$, respectively. After introducing the inverse proton cyclotron frequency $\omega_{cp} := eB_0/m_p$ as a natural time scale and the ion inertial length $d_i = c/\omega_{pp}$ as natural length scale the dimensionless electric field $\boldsymbol{e} := \boldsymbol{E}/cB_0$ has the following form

$$\begin{aligned} e_{SLy} &= (V_{SL}/c) b_{\max} \cdot g(\xi) \\ e_{SLz} &= -(V_{SL}/c) b_{\max} p \cdot f(\xi) . \end{aligned} \quad (3)$$

Concerning the x-component of the electric field the induction law gives no information because of the structure of this equation and our assumption that the field varies only with x (and t). Furthermore the integration constants appearing in the computation of the the e_y- and e_z-component have been chosen in such a way that $\boldsymbol{e} \equiv \boldsymbol{0}$ is obtained outside the SLAMS.

The e_x-component can be estimated analysing the plasma flow at SLAMS. As already mentioned in Sect. 2 the plasma flow inside a single SLAMS is only gradually decelerated. The flow speed of protons inside the SLAMS can be estimated using continuity equation. If we assume a steady plasma flow, the flow speed outside (index o) and inside (index i) the SLAMS is related via $\rho_o u_{ox} = \rho_i u_{ix}$. Thus, we obtain for the difference in the kinetic energy of a single proton inside and outside the SLAMS of

$$\Delta W = (1/2) m_p (u_{ox}^2 - u_{ix}^2) = (1/2) m_p u_{ox}^2 (1 - (\rho_o/\rho_i)^2) \quad (4)$$

For a starting velocity of $u_{ox} = 5V_A$, which is a typical plasma flow speed at SLAMS, and with a density compression range of $1.5\rho_o \leq \rho_i \leq 3.1\rho_o$ the energy difference is $7 m_p V_A^2 \leq \Delta W \leq 11 m_p V_A^2$.

On the other hand, if we analyse the particle trajectory of a single proton penetrating a SLAMS given by Eqs. 2 and 3 with $e_{SLx} = 0$ we find a deceleration from $v_{ox} = 5V_A$ to roughly $v_{ix} = 1V_A$. This results in a difference of kinetic energy of $\Delta W_{\text{test}} = 12 m_p V_A^2$. The difference between the energy losses calculated from continuity equation and test particle approach can be balanced introducing an electric potential inside the SLAMS via $e\Delta\Phi = \Delta W_{\text{test}} - \Delta W$. Thus, we find an electric potential in the range $1 m_p V_A^2 \leq e\Delta\Phi \leq 5 m_p V_A^2$. This potential is correlated with an electric field in the x-direction $E_x = -\partial_x \Phi$ acting over a distance of roughly $L = 10 d_i$ (the typical SLAMS scale length, cf. Fig. 3). The corresponding electric field in dimensionsless quantities can be estimated via $e_x = E_x/(cB_0) \approx -(\Delta\Phi/L)(1/cB_0)$, i.e.,

$$e_{SLx}(\xi) \approx \frac{1}{cB_0}\frac{\Delta\Phi}{10 d_i} \leq 5 \frac{m_p}{eB_0}\frac{V_A^2}{10 c d_i} = 0.5 \frac{V_A}{c}\frac{V_A}{\omega_{cp} d_i} . \quad (5)$$

With $\omega_{cp} d_i = B_0/(\mu_0 m_p N_e)^{1/2} = V_A$ as the Alfvén velocity we obtain a e_{SLx}-component smaller than $0.5(V_A/c)$. In comparision to this value the e_y-component from Eq. 3 is about $10(V_A/c)$, obtained by setting $V_{SL} = 5V_A$ and a mean value of about 2 for the quantity $b_{\max} g(\xi)$ (cf. Fig. 3). Thus, the e_{SLx}-component is one or two orders of magnitude smaller than the e_y- and e_z-component in Eq. 3. For this reason we will neglect the effects of the e_x-component.

Since we are mainly interested in electron acceleration at coronal shock waves in order to explain the observed solar type II radio bursts the plasma parameters in the solar corona at the 90 MHz plasma level are briefly summarized (cf. Mann et al. 1995). Assuming that the radio emission at the fundamental band of type II bursts (cf. Fig. 1) occurs at the electron plasma frequency $\omega_{pe} = ((e^2 N_e)/(m_e \epsilon_0))^{1/2}$ the particle number density of the electrons is given by $N_e = 10^{14}\,\text{m}^{-3}$. Assuming a fourfold Newkirk model above active regions (Newkirk 1961) the 90

MHz plasma level is located at roughly $0.6R_\odot = 420,000$ km above the photosphere. The magnetic field in such heights can be estimated by an empirically determined formula given by Dulk & McLean (1978) resulting in a magnetic field strength of about 1 G. Thus, the natural units introduced before can be assumed to $d_i = 30$ m, $\omega_{cp} = 9.6 \cdot 10^3\,\mathrm{s}^{-1}$ and $V_A = 280$ km/s at the 90 MHz level in the solar corona. Furthermore, we will adopt a coronal temperature of $T = 2 \cdot 10^6$K.

Adding $e_{SLx} = 0$ to Eq. 3 the equation of motion (Eq. 1) was solved for the modelled magnetic field from Fig. 3 using a Runge-Kutta method for ordinary differential equations (e.g. Press et al. 1992). The results for the particle velocity parallel to the local magnetic field $v_\parallel$ and for the "magnetic moment" $m_M := m_e v_\perp^2/2B$ are depicted in Fig. 4. The equation of motion was solved for an electron starting at the right hand side of the SLAMS using the aforementioned natural scale lengths, i.e., ω_{cp}, d_i and V_A. Note, that $v_\parallel$ and m_M are depicted as functions of the particle position inside the SLAMS, i.e., the electron starts at the right hand side of each panel. Under the coronal conditions mentioned above the electron velocity within the SLAMS rises from a thermal value of $v_{\mathrm{therm}} = (k_B T/m_e)^{1/2} = 20V_A = 5,500$ km/s up to about $300V_A = 0.3c$. This justifies the non relativistic treatment of the equation of motion. Leaving the SLAMS the velocity $v_\parallel$ goes back to roughly $100V_A = 28,000$ km/s. During this acceleration process the electron energy is growing from a thermal value of 0.1 keV to an energy of 20 keV inside the SLAMS in an acceleration time of $t_{\mathrm{acc}} = 4.1\omega_{cp}^{-1} = 2.5 \times 10^{-5}$ s. On the other hand the value of the magnetic moment stays nearly constant. In order to get a better understanding of the physics of this acceleration process we are now going to discuss a simplified analytical approach to our test particle calculations.

The behaviour of magnetic moment defined above can easily be understood if we review some results from adiabatic theory (e.g. Northrop 1963). There it is shown that for particle movements in slowly changing magnetic fields, i.e., $r_L|\nabla b/b| \ll 1$ and $\omega_c^{-1}|\partial b/b\partial t| \ll 1$ the magnetic moment is a so-called adiabatic invariant. $r_L := v_\perp/\omega_c$ is the Larmor radius of the gyrating particle. For thermal electrons under coronal conditions the Larmor radius is roughly 0.3 m, while the magnetic field changes on scales of several times the ion inertial length (30 m), so that adiabatic theory can be employed.

In adiabatic theory the particle motion is subdivided into the motion of the particle's guiding center and into the particle's gyration (e.g. Northtrop 1963). Thus, the change in kinetic energy $dW/dt = \boldsymbol{F}\cdot\boldsymbol{v} = -e\boldsymbol{E}\cdot\boldsymbol{v}$ during the passage of a SLAMS can be written as

$$\frac{dW}{dt} = -e\left(\frac{dR_\parallel}{dt}E_\parallel + \frac{d\boldsymbol{R}_\perp}{dt}\cdot\boldsymbol{E}_\perp\right) + \frac{dW_{\mathrm{rot}}}{dt} \tag{6}$$

if we assume $\boldsymbol{v} = \dot{R}_\parallel\hat{\boldsymbol{b}} + \dot{\boldsymbol{R}}_\perp + \dot{\boldsymbol{r}}'$ ($\dot{} = d/dt$), with $\dot{R}_{\parallel,\perp}$ as guiding center velocity along and across the local magnetic field, respectively. The last term is the pure gyromotion of the particle around the (moving) guiding center. The same indices denote the electric field components parallel and perpendicular to the local magnetic field and W_{rot} is the gyrating kinetic energy of the electron corresponding to $-e\boldsymbol{E}\cdot\dot{\boldsymbol{r}}'$.

The particle's energy gain can be estimated neglecting the second and third term on the right hand side of Eq. 6 in comparision with the first term. This can be shown setting $p = 0$ in Eq. 2 and 3 with the result that the velocity gain of the electron is about ten times V_A. The physical reasons for this behaviour are small gradients in the magnetic field, slight bending of the magnetic field lines (responsible for the guiding center drift perpendicular to the direction of the magnetic field) and the invariance of the magnetic moment (by which the change in the gyrating energy is limited). From this point of view the electron accelerating mechanism differs from the well known shock drift acceleration: For the latter the energy gain is caused by an electron drift perpendicular to the magnetic field in the direction of $\boldsymbol{E}_\perp$, i.e., the second term on the right hand side of Eq. (6) is responsible for shock drift acceleration. For the mechanism presented in this paper the electrons gain energy because of an electric field component in the direction of the magnetic field, i.e., the first term on the right hand side of Eq. (6) represents a locally acting linear accelerator.

In order to study the motion along the local magnetic field we substitute $\dot{R}_\parallel = (B/B_x)(dx/dt)$, i.e., we study a projection of the guiding center motion to the x-axis. Now Eq. 6 can be solved as a function of the particle's guiding center position x within the SLAMS

$$\frac{m_e}{2}[v_\parallel^2(x_1) - v_\parallel^2(x_0)] = -e\int_{x_0}^{x_1}\frac{\boldsymbol{E}\cdot\boldsymbol{B}}{B}\frac{B}{B_x}\,dx\,. \tag{7}$$

Using the aforementioned natural units to obtain dimensionless quantities the energy gain can be written as (see Eqs. 2 and 3)

$$v_\parallel^2(x_1) - v_\parallel^2(x_0) = 2V_{SL}\tan\psi\frac{m_p}{m_e}\int_{x_0}^{x_1} b_y(x)\,dx\,. \tag{8}$$

This behaviour of the electron velocity is in very good agreement with the numerical solution (cf. Eqs. 1, 2 and 3) of the particle trajectories in Fig. 4. For an electron starting at the right hand side of the SLAMS depicted in Fig. 3 the definite integral $\int_{x_0}^{x_1} b_y\,dx$ is positive as long as $x_1 > 0$. This follows from the fact that both b_y and the path element dx are negative so that the electrons gain energy. For $x_1 < 0$ the electrons lose energy causing a deceleration of the particle as depicted in Fig. 4. For an electron starting at the left hand side of the SLAMS from Fig. 3 the energy rises as long as $x_1 < 0$ because b_y and dx are positive in this area. For $x_1 > 0$ the electron is decelerated. Thus, the energy gain can simply be approximated by a numerical integration of the b_y-component from Eq. 2, i.e., the electron acceleration is determined by the noncoplanar component of the magnetic field.

Here it should be mentioned that an electron acceleration occurs only for a b_y-component as depicted Fig. 3 or $-1 \le p < 0$ in Eq. 2. For $0 < p \le 1$ the electrons encountering the SLAMS are first decelerated and then they are accelerated (if their starting energy was high enough) or are reflected. Furthermore, it

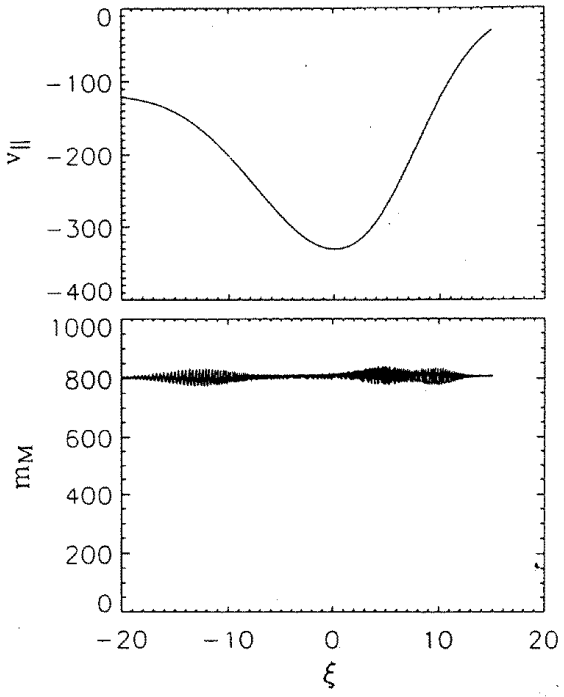

Fig. 4. Electron velocity parallel to the local magnetic field and behaviour of the "magnetic moment" for an electron penetrating the SLAMS from Fig. 3 as a function of the particle position inside the SLAMS. The spatial dimension is normalized to the ion inertial length and to the Alfvén velocity, the magnetic moment is depicted in arbitrary units. The electron starts with a thermal velocity of about 40 at the right side (at ξ = 15) and ends with a velocity of about 120, while the magnetic moments stays nearly constant.

can be seen from Eq. 8, that the velocity gain vanishes, if the SLAMS propagate exactly along the ambient magnetic field (ψ = 0). Thus, the basic ingredients of the acceleration mechanism presented in this section are the noncoplanar magnetic field component of SLAMS and their ability to propagate at an oblique angle to the background magnetic field. Both properties are well established in the observations of SLAMS (Mann et al. 1994) and in hybrid simulations of this structures (Kucharek & Scholer 1991).

The velocity gain of the electrons leaving the SLAMS can be obtained evaluating the definite integral $\int_{x_0}^{x_1} b_y\,dx$ with integration boundaries outside the SLAMS. If $\int_{x_0}^{x_1} b_y\,dx > 0$ the electrons starting at the right hand side of the SLAMS (at x_0) are able to leave the SLAMS on the left side with a velocity which is greater than the starting velocity (left side in the upper panel of Fig. 4). Electrons starting from the left side are not able to get through the SLAMS; they get stuck in the right side at x_r, where $\int_{x_0}^{x_r} b_y\,dx$ = 0, are subsequently reflected and leave the SLAMS on the left side again. If $\int_{x_0}^{x_1} b_y\,dx < 0$ the electrons from the right side are reflected and the electrons encountering from the left side leave the SLAMS with a higher energy than their starting energy. In case of $\int_{x_0}^{x_1} b_y\,dx$ = 0 electrons entering the SLAMS from both sides are only accelerated inside and leave the SLAMS with a velocity equal to the starting value.

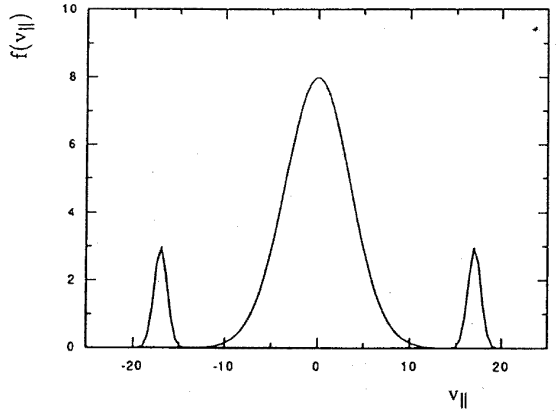

Fig. 5. Distribution function of electrons at a fixed position within a single SLAMS.

4. Discussion

As already mentioned in the introduction solar type II radio are regarded as the radio signature of supercritical, quasi-parallel shock waves in the solar corona. In order to find out whether the accelerated electrons described in the previous section are able to generate radio waves via the excitation of Langmuir or upper hybrid waves the distribution function of the accelerated electrons must be examined.

As a necessary condition for the generation of a plasma instability we need a distribution function $f_e(\boldsymbol{v})$ of suprathermal electrons with either $\partial f_e/\partial v_\parallel > 0$ (beam instability) or $\partial f_e/\partial v_\perp > 0$ (loss-cone instability) in a velocity interval around the phase speed of the plasma waves under consideration (e.g. Krall & Trivelpiece 1986).

Now, the electron distribution function obtained by the acceleration process from Sect. 3 has the following properties (see Fig. 5). We expect a distribution of electrons consisting of two beam-like bumps superimposed on a Maxwellian background distribution, which is assumed to be the undisturbed distribution in the coronal plasma. The first peak (the left one with $v_\parallel < 0$) arises from electrons penetrating the SLAMS from the right hand side (cf. Fig. 4). The second peak is due to accelerated electrons which encounter the SLAMS from the left, i.e. electrons approaching the SLAMS from both sides are accelerated within it (see Eq. 8).

Eq. 8 shows furthermore that the position of the peak in velocity space depends on the depth of penetration into the SLAMS, i.e. the distribution function is of the form $f_e(\boldsymbol{v}, \boldsymbol{x})$. In order to get more information about this function we need a detailed description of the noncoplanar magnetic field component b_y, which is out of the scope of the present paper.

An estimation of the fraction of accelerated electrons inside the SLAMS can be achieved using two-fluid theory of the plasma within the SLAMS region. In this description the ratio $\nu := (N_e - N_p)/N_e$ is conversely proportional to the square

of the length scale L of the examined structure (e.g. Krall & Trivelpiece 1986)

$$\nu \propto \lambda_D^2 / L^2 \tag{9}$$

with $\lambda_D = (k_B T_e/m_e)^{1/2}/\omega_{pe}$ as Debye length of the plasma. Under coronal conditions the Debye length is in the order of 10^{-2} m, the typical length of a SLAMS about 300 m resulting in a ratio $\nu \approx 10^{-9}$.

In order to satisfy the aforementioned necessary condition for the generation of plasma instabilities the fraction ν of accelerated electrons must exceed the Maxwellian background. In a Maxwellian plasma the number of particles in the velocity interval $[v_\parallel, v_\parallel + dv_\parallel]$ is (in units of the thermal particle velocity $v_{\rm therm} = (k_B T/m_e)^{1/2}$)

$$\mathrm{d}N_e(v_\parallel) = N_e \frac{1}{\sqrt{2\pi}} \exp(-v_\parallel^2/2)\,\mathrm{d}v_\parallel\,. \tag{10}$$

Demanding that the number of suprathermal electrons νN_e exceeds this Maxwellian part for example a thousand times we find that the accelerated elctrons must have a velocity of about $7.3 v_{\rm therm} \approx 130 V_A$ (under coronal conditions). In this region the Maxwellian distribution has a value of $\mathrm{d}N_e(v_\parallel = 7.3) = 10^{-12} N_e\,\mathrm{d}v_\parallel = 10^{-3}\nu N_e\,\mathrm{d}v_\parallel$.

Thus, we can assume that the population of suprathermal electrons with a distribution similar to Fig. 5 is able to produce an enhanced Langmuir turbulence inside the SLAMS. An experimental evidence for this conclusion may be found in the observation of an enhanced Langmuir turbulence at some quasi-parallel shocks in the interplanetary medium reported by Thejappa et al. (1995). Assuming the same scenario in the solar corona we get the following picture for the production of solar type II radio bursts. As already mentioned in Sect. 2 SLAMS are not only characterized by a compression of the magnetic field but are also accompanied by an enhancement of the plasma density. The statistical analysis of SLAMS at Earth's bow shock yields a density compression of $N_{eSL}/N_{e0} = 2.3 \pm 0.8$ (N_{eSL}, maximal electron number density inside the SLAMS and N_{e0}, background plasma density) (Mann et al. 1994). This means on the other hand that the local plasma frequency varies inside the SLAMS according to $\omega_{pe} \propto N_e^{1/2}$. Assuming that supercritical, quasi-parallel shock waves in the solar corona consist of SLAMS with a similar density compression, we get an instantaneous bandwidth in the order of

$$\frac{\Delta f}{f} \approx \sqrt{\frac{N_{eSL}}{N_{e0}}} - 1 \approx 0.52\,, \tag{11}$$

if we take the mean value of the measured density jump at SLAMS. This instantaneous bandwidth is in good agreement with the statistical analysis of the distribution of the bandwidth of solar type II radio bursts (we found $(\Delta f/f)_{\rm sol} = 0.32 \pm 0.08$, see Mann et al. 1995) and with the instantaneous bandwidth of interplanetary type II bursts of $(\Delta f/f)_{\rm int} = 0.5 \pm 0.3$ (Lengyel-Frey & Stone 1989). Furthermore our analysis provides the possibility to understand the observed backbone fine structures. Taking the production of radio waves in more than one SLAMS into consideration, solar type II bursts should be regarded as a patchword of slowly drifting (according to a rising shock wave in the corona) "clouds" of enhanced radio emission representing the suprathermal populations of accelerated electrons inside single SLAMS (cf. Fig. 1). Furthermore, these clouds should show fast drifting fine structures, which are also visible in Fig. 1. In order to obtain the typical time scales of the observed solar type II radio bursts of several minutes we need a permanent process of creation of ULF-waves, steepening into SLAMS and decay of this structures (see e.g. Schwartz & Burgess 1991). This process becomes necessary if we take the typical stable phases of SLAMS into consideration. According to the computer simulations of Scholer (1993) SLAMS appear and vanish upon a time scale of about 100 times the inverse proton cyclotron frequency; this means a time of about 0.01 s under coronal conditions. On the other hand the time scale for accelerating electrons within a single SLAMS is of the order of $2.5 \cdot 10^{-5}$ s.

Finally, it should be mentioned that the acceleration mechanism presented here provides highly energetic electrons only in a spatially limited region, leading to the finite bandwidth of the backbone of the observed type II bursts. In order to explain the suprathermal electron population generating the herringbones structures we need either a noncoplanar magnetic field with $\int_{x_0}^{x_1} b_y\,dx \neq 0$ or another electron acceleration mechanism, e.g. the mirror mechanism described in an earlier paper (Mann & Claßen 1995).

5. Summary and conclusions

In this paper we presented a mechanism for the acceleration of electrons at substructures of supercritical, quasi-parallel shock waves using test particle computations in given electric and magnetic fields.

The behaviour of the magnetic field of this so-called SLAMS has been extracted from in-situ magnetometer-measurements at Earth's bow shock. Instead of real measured field data we took a mathematically modelled SLAMS reflecting the essential behaviour of real existing SLAMS. The physical reason for this approach is a description of SLAMS in form of simple MHD-waves. The corresponding electric field was calculated from the modelled magnetic field using the induction equation.

First, the test particle calculations were performed for an explicit mathematical realization of a single SLAMS solving the complete equation of motion with numerical methods. Here we found an electron acceleration up to velocities in the order of several hundred times the Alfvén velocity. Secondly, we used an analytical approach using adiabatic theory, i.e., solving a reduced equation of motion for the particle's guiding center and neglecting the gyromotion. The results showed that the aforementioned acceleration is caused by the noncoplanar magnetic field component of the SLAMS. The energy gain of electrons can be estimated by a simple numerical integration of the noncoplanar magnetic field component.

We discussed the possibility for an indirect evidence of the suprathermal electrons by means of remote sensing techniques.

Under the assumption that SLAMS are basic ingredients of supercritical, quasi-parallel shock in the solar corona we showed that the resulting nonthermal distribution functions are able to produce plasma instabilities inside single SLAMS. Taking the density compression of SLAMS into account the corresponding variation of the electron plasma frequency allowed us to reduce the patchy fine structures of the backbone of solar type II radio bursts to accelerated electrons in a patchwork of SLAMS at supercritical, quasi-parallel shock waves.

References

Axford W.I., Leer E., Skadron G., 1977, Proc. 15th Int. Cosmic Ray Conf., 11, 132

Auraß H., 1992, Ann.Geophys., 10, 359

Benz A.O., Thejappa G., 1988, A&A, 202, 267

Bougeret J.L., 1985, in Tsurutani B.T., R.G. Stone R.G. (eds.) Collisionless Shocks in the Heliosphere: Reviews of Current Research, AGU GN-35, Washington DC, p. 13

Cairns I.H., 1986, J.Geophys.Res., 91, 2975

Decker R.B., 1988, Sp.Sc.Rev., 48, 193

Dulk G.A., McLean D.I., 1978, Sol. Phys., 57, 279

Fermi E., 1949, Phys.Rev., 75, 1149

Filbert P.C., Kellog P.J., 1979, J.Geophys.Res., 84, 1369

Greenstadt E.W., Green J.M., Inouye G.T. et al., 1970, Cosmic Electrodyn., 1, 160

Gurnett D.A., 1995, Solar Wind 8, in press

Holman G.D., Pesses M.E., 1983, ApJ, 267, 837

Hoppe M.M., Russell C.T., Frank L.A., Eastman T.E., Greenstadt E.W., 1981, J.Geophys.Res., 86, 4471

Kennel C.F., Edmiston J.P., Hada T., 1985, in Tsurutani B.T., Stone R.G. (eds.) Collisionless Shocks in the Heliosphere: Reviews of Current Research, AGU GN-34, Washington DC, p. 1

Krall N.A., Trivelpiece A.W., 1986, Principles of Plasma Physics, McGraw-Hill, New York

Krüger A., 1979, Introduction to Solar Radioastronomy and Radio Physics, Reidel, Dordrecht, NL

Kucharek H., Scholer M., 1991, J.Geophys.Res., 96, 21195

Lengyel-Frey D., Stone R.G., 1989, J.Geophys.Res., 94, 159

Leroy M.M., Mangeney A., 1984, Ann.Geophys., 2 (4), 449

Lühr H., Klöcker N., Oelschlägel W., Häusler B., Acuna M., 1985, IEEE Trans.Geosci.Remote Sens., GE-23, 259

Malara F., Elaoufir J., 1991, J.Geophys.Res., 96, 7641

Mann G., 1995a, in Benz A.O., Krüger A. (eds.) Coronal Magnetic Energy Release, Springer, Berlin, Heidelberg, p. 183

Mann G., 1995b, J.Plasma.Phys., 53, 109

Mann G., Claßen H.-T., 1995, A&A, 304, 576

Mann G., Claßen H.-T., Auraß H., 1995, A&A, 295, 775

Mann G., Lühr H., Baumjohann W., 1994, J.Geophys.Res., 99, 13315

Nelson G.S., Melrose D.B., 1985, in McLean D.J., Labrum N.R. (eds.) Solar Radiophysics, Cambridge Univ. Press, Cambridge, UK, p. 333

Newkirk G.A., 1961, ApJ, 133, 983

Northrop T.G., 1963, The Adiabatic Motion of Charged Particles, Wiley Interscience, New York

Paschmann G., Sckopke N., Bame S.J. et al., 1979, Geophys.Res.Lett., 6, 209

Press W.H., Teukolsky S.A., Vetterling W.T., Flannery B.P., 1992, Numerical Recipes in Fortran: The Art of Scientific Computing, Cambridge

Roberts J.A., 1959, Austr.J.Phys., 12, 327

Scholer M., 1993, J.Geophys.Res., 98, 47

Scholer M., Fujimoto M., Kucharek H., 1992, ESA SP-346, 59

Schwartz S.J., Burgess D., 1991, Geophys.Res.Lett., 18, 373

Schwartz S.J., Burgess D., Wilkinson W.P. et al., 1992, J. Geophys. Res., 97, 4209

Schwartz S.J., Kessel R.L., Brinca C.C. et al., 1988, J. Geophys. Res., 93, 11295

Thejappa G., Wentzel D.G., MacDowall R.J., Stone R.G., 1995, Geophys.Res.Lett., 22, 3421

Thomsen M.F., Gosling J.T., Bame S.J., Russel C.T., 1990, J. Geophys. Res., 95, 957

Treumann, R.A., Bauer, O.H., LaBelle, J. et al., 1986, Adv.Sp.Res., 6, 93

Wu C.S., 1984, J.Geophys.Res., 89 (A10), 8857

This article was processed by the author using Springer-Verlag LaTeX A&A style file *L-AA* version 3.